Coherent optical spectroscopy of a single quantum dot using photon counting statistics

Yonggang Peng (彭勇刚) and Yujun Zheng (郑雨军)*
School of Physics, Shandong University, Jinan 250100, China
(Received 17 March 2009; published 23 October 2009)

We present the theory of coherent optical spectroscopy for single quantum dot under the pump-probe driving. We generally study the line shapes, Mandel's Q parameters, and few photon emission probabilities of single quantum dot system. The probe signals demonstrate the Autler-Townes splitting effect, and the first moment of our results confirms recent experimental results [Xu *et al.*, Science **317**, 929 (2007)]. We show that the pump and probe fields modify the emission photon statistical properties and control emission photon properties.

DOI: 10.1103/PhysRevA.80.043831 PACS number(s): 42.50.Ar, 78.67.Hc, 78.47.Fg

Due to the advances of semiconductor growth, semiconductor dots [quantum dots (QDs)], have been widely investigated as potential technology-compatible quantum light emitters. The various properties, for example, quantum beats [1], coherent population trapping [2], Rabi oscillations [3], entanglement photon pairs, some other quantum interference phenomena [4–8], etc., have been investigated extensively. Recent studies suggest that QDs could offer the potential to be used as elements in optoelectronics and quantum logic devices [9]. As is known, when a two-level system is driven by a strong pump field, we can use a field to probe the excited state (or the ground state with another auxiliary state). The probe signals demonstrate the well known Autler-Townes splitting, which first observed on radio frequency in 1955 [10]. Since then several groups observed the Autler-Townes splitting in the gas phase molecules [11–14]. Sun and Lou demonstrated the Autler-Townes splitting of Na_2 molecule using the evolution of the wave package approach [14]. Recently, Xu *et al.* investigated single QDs driven simultaneously by pump-probe field; their experimental results show that the Autler-Townes splitting and Mollow splitting can be obtained by probing absorption spectra [9].

The recent experiment on the coherent optical spectroscopy of single quantum dots inspires some theoretical questions and shows theoretical challenges. In this paper, we report a theoretical approach to get the coherent optical spectroscopy of single quantum dots driven by pump-probe field. We show how this approach be used to control the statistical properties of emission photons of single QDs. In contrast with previous approaches, our theory enables studies of high order of cumulants and other physical variables, such as the photon emission probabilities and the distribution of waiting time of photon emission events.

We generally consider single quantum dots modeled by the V-type three-level system with two electric dipole moments $\boldsymbol{\mu}_{12}$ and $\boldsymbol{\mu}_{13}$ under driving by pump and probe fields simultaneously. The schematic diagram is shown in Fig. 1. In our treatment, the pump field couples with the ground state $|1\rangle$ and excited state $|3\rangle$ and the probe field couples with the ground state $|1\rangle$ and excited state $|2\rangle$ under the dipole moment approximation. We concentrate on the probe signals which correspond to the emission photons of the system caused by the probe field (as usual, we denote them as x-polarized photons). We assume that the transitions between the ground state and the excited states are electric dipole allowed, but the direct transition between the two excited states is electric dipole forbidden. The pump and probe fields are described in semiclassical form, $\boldsymbol{E}_{pump}(t)=\mathcal{E}_{pump}\cos(\omega_{pump}t)$, $\boldsymbol{E}_{probe}(t)=\mathcal{E}_{probe}\cos(\omega_{probe}t)$.

The system evolution with time is described using density matrix, and the density matrix of the system satisfies the quantum Liouville equation [15,16],

$$i\hbar\frac{\partial}{\partial t}\rho(t)=[\mathcal{H},\rho(t)], \tag{1}$$

where the Hamiltonian is

$$\mathcal{H}=\mathcal{H}_s+\mathcal{H}_R+\mathcal{H}_{sR}+\mathcal{V}. \tag{2}$$

$\mathcal{H}_s$ is the Hamiltonian of bare single quantum system, $\mathcal{H}_R$ is the Hamiltonian of quantized vacuum field, $\mathcal{H}_{sR}$ is the interaction between the system and the vacuum field, and $\mathcal{V}$ is the interaction between the system and the external field (including pump field and probe field). They are $\mathcal{H}_s=\Sigma_{n=1}^{3}\hbar\omega_n|n\rangle\langle n|$, $\mathcal{H}_R=\Sigma_{\boldsymbol{k}\lambda}\hbar\omega_k(a^{\dagger}_{\boldsymbol{k}\lambda}a_{\boldsymbol{k}\lambda}+\frac{1}{2})$, $\mathcal{H}_{sR}=-i\Sigma_{mn;\boldsymbol{k}\lambda}\hbar g^{(mn)}_{\boldsymbol{k}\lambda}\{a_{\boldsymbol{k}\lambda}e^{-i\omega_k t}-a^{\dagger}_{\boldsymbol{k}\lambda}e^{i\omega_k t}\}|m\rangle\langle n|$, and $\mathcal{V}=-\boldsymbol{\mu}\cdot\boldsymbol{E}(t)$. $g^{(mn)}_{\boldsymbol{k}\lambda}=\sqrt{(\omega_k/2\varepsilon_0 V\hbar)}\boldsymbol{\mu}_{mn}\boldsymbol{e}_{\boldsymbol{k}\lambda}$ is the coupling constant of the system and the vacuum field. Introducing the reduced density matrix $\sigma(t)=\mathrm{Tr}_R\{\rho(t)\}$, the evolution of the reduced density

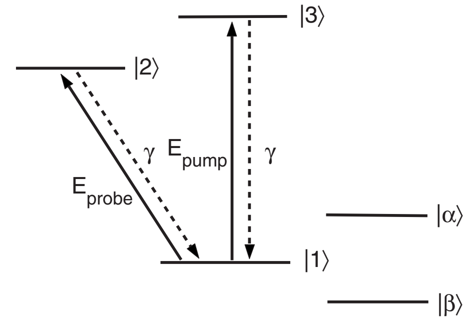

FIG. 1. The schematic diagram of the V-type three-level system.

*yzheng@sdu.edu.cn

matrix elements can formally written, in Liouville space, as [16]

$$\dot{\sigma}_{ij}(t) = \mathcal{L}_{ij;kl}\sigma_{kl}. \tag{3}$$

We can partition the Liouville operator into two parts, i.e., $\mathcal{L}_{ij;kl}=\mathcal{L}^{(x)}_{ij;kl}+\mathcal{L}'_{ij;kl}$. $\mathcal{L}^{(x)}_{ij;kl}=2\gamma_2|2\rangle\langle 2|$ describes the transition from the excited state $|2\rangle$ into the ground state $|1\rangle$ with the spontaneous emission rate γ_2, where $\gamma_{ijkl}=\boldsymbol{\mu}_{ij}\cdot\boldsymbol{\mu}_{kl}(|\omega_{kl}|^3/6\varepsilon_0\hbar\pi c^3)$ is the damping constants (in short, we note $\gamma_k=\gamma_{k11k}$, $\gamma_{ij}=\gamma_{i11j}$) and $\omega_{ij}=\omega_i-\omega_j$ is the frequency difference of the states $|i\rangle$ and $|j\rangle$. $\mathcal{L}'_{ij;kl}$ is the portion of $\mathcal{L}_{ij;kl}$ not pulled out in $\mathcal{L}^{(x)}_{ij;kl}$. The photon statistics can be obtained from the solution of Eq. (3) in terms of an iterative expansion in $\mathcal{L}^{(x)}_{ij;kl}$. However, it is convenient to proceed by defining the generating function as [17–19] $\mathcal{G}_{ij}(s,t)=\sum_{n=0}^{\infty}\sigma^{(n)}_{ij}s^n$, where the $\sigma^{(n)}_{ij}$ represents that the system has emitted n photons in time interval $[0,t]$. Further, we introduce the generalized Bloch vectors $\mathcal{U}_1=\mathrm{Re}(\mathcal{G}_{12})$, $\mathcal{V}_1=\mathrm{Im}(\mathcal{G}_{12})$, $\mathcal{U}_2=\mathrm{Re}(\mathcal{G}_{13})$, $\mathcal{V}_2=\mathrm{Im}(\mathcal{G}_{13})$, $\mathcal{U}_3=\mathrm{Re}(\mathcal{G}_{23})$, $\mathcal{V}_3=\mathrm{Im}(\mathcal{G}_{23})$, $\mathcal{W}_1=(\mathcal{G}_{22}-\mathcal{G}_{11})/2$, $\mathcal{W}_2=(\mathcal{G}_{33}-\mathcal{G}_{11})/2$, and $\mathcal{Y}=\mathcal{G}_{11}+\mathcal{G}_{22}+\mathcal{G}_{33}$.

We can, in the rotating wave approximation (RWA) and employing the above definitions and Eq. (3), derive the evolution equations of the generalized Bloch vectors as $\dot{\mathbf{Y}}=\mathbf{MY}$. The vector $\mathbf{Y}=(\mathcal{U}_1,\mathcal{V}_1,\mathcal{W}_1,\mathcal{U}_2,\mathcal{V}_2,\mathcal{W}_2,\mathcal{U}_3,\mathcal{V}_3,\mathcal{Y})^{\dagger}$; the coefficient matrix $\mathbf{M}$ is

$$\mathbf{M}=\begin{pmatrix}
-\gamma_2 & \Delta_1 & 0 & -\gamma_{23} & 0 & 0 & 0 & -\Omega_{13}/2 & 0\\
-\Delta_1 & -\gamma_2 & -\Omega_{12} & 0 & -\gamma_{23} & 0 & -\Omega_{13}/2 & 0 & 0\\
0 & \Omega_{12} & -4\gamma_2(1+s)/3+2\gamma_3/3 & 0 & \Omega_{13}/2 & 2\gamma_2(1+s)/3-4\gamma_3/3 & -3\gamma_{23} & 0 & -\gamma_2(1+s)/3-\gamma_3/3\\
-\gamma_{23} & 0 & 0 & -\gamma_3 & \Delta_2 & 0 & 0 & \Omega_{12}/2 & 0\\
0 & -\gamma_{23} & 0 & -\Delta_2 & -\gamma_3 & -\Omega_{13} & -\Omega_{12}/2 & 0 & 0\\
0 & \Omega_{12}/2 & -4\gamma_2 s/3+4\gamma_3/3 & 0 & \Omega_{13} & 2\gamma_2 s/3-8\gamma_3/3 & -3\gamma_{23} & 0 & -\gamma_2 s/3-2\gamma_3/3\\
0 & \Omega_{13}/2 & -2\gamma_{23}/3 & 0 & \Omega_{12}/2 & -2\gamma_{23}/3 & -(\gamma_2+\gamma_3) & \Delta_2-\Delta_1 & -2\gamma_{23}/3\\
\Omega_{13}/2 & 0 & 0 & -\Omega_{12}/2 & 0 & 0 & -(\Delta_2-\Delta_1) & -(\gamma_2+\gamma_3) & 0\\
0 & 0 & 8\gamma_2(s-1)/3 & 0 & 0 & -4\gamma_2(s-1)/3 & 0 & 0 & 2\gamma_2(s-1)/3
\end{pmatrix}, \tag{4}$$

where $\Delta_1=\omega_{probe}-\omega_{21}$ and $\Delta_2=\omega_{pump}-\omega_{31}$ are the detuning frequencies of the probe and pump field and $\Omega_{12}=-\boldsymbol{\mu}_{12}\cdot\mathcal{E}_{probe}/\hbar$ and $\Omega_{13}=-\boldsymbol{\mu}_{13}\cdot\mathcal{E}_{pump}/\hbar$ are the Rabi frequencies of the probe and pump fields, respectively. The related physical variables can be extracted from the generating functions, such as the photon emission counting moments, $\langle N^{(m)}\rangle(t)\equiv\langle N(N-1)\cdots(N-m+1)\rangle(t)=(\partial^m/\partial s^m)\mathcal{Y}(s,t)|_{s=1}$, the probability of emission n photons in the time interval $[0,t]$, $p_n(t)=\frac{1}{n!}(\partial^n/\partial s^n)\mathcal{Y}(s,t)|_{s=0}$, etc. Then we can get line shape and Mandel's Q parameter as $I(\omega)=\frac{d}{dt}\langle N^{(1)}\rangle(t)$ for long time and $Q=(\langle N^{(2)}\rangle-\langle N^{(1)}\rangle^2)/\langle N^{(1)}\rangle$, respectively.

For concreteness, we consider InAs self-assembled quantum dots. This system is studied in experiment recently [9]. To compare with the experimental results, we consider the same case with the experiment, namely, the system is driven by orthogonal polarized cw pump and probe fields and $\gamma_3=\gamma_2=\gamma$, $\gamma_{23}=0$. The line shapes and Mandel's Q parameters of the x-polarized photons (probe signals) as a function of the detuning frequency of the probe field Δ_1 are shown in the top panel of Fig. 2 for the different strengths of pump field (they are noted in the figure) in the case of the pump field at resonance (i.e., $\Delta_2=0$). The red dots are the experimental results in Ref. [9]. At the absent pump field, the x-polarized photon shows a resonance peak at position $\Delta_1=0$, which is the same as a simple two-level system. As the pump field increases, the resonance peak of the x-polarized photon shows the Autler-Townes splitting. In this case, the ground state $|1\rangle$ dressed by the pump field, and it splits into two substates $|\alpha\rangle$ and $|\beta\rangle$ [we assume that the energy level of state $|\alpha\rangle$ is higher than that of state $|\beta\rangle$ (see Fig. 1)]. The reason for the splitting is well described by dressed state theory [15]. Mandel's Q parameters reflect the antibunching behaviors of the x-polarized photons. From the figure, we can know, the pump field strength decides the position of the peak (i.e., the splitting of the dressed states $|\alpha\rangle$ and $|\beta\rangle$), and it does not affect the properties of the x-polarized photons, that is, the emission photons for all the pump field strengths here show the antibunching effects. Also, Mandel's Q parameters have the similar values except for the case of absent pump field.

The bottom panel of Fig. 2 demonstrates the line shapes and Mandel's Q parameters for different detuning frequencies of the pump field (the detuning frequencies are noted in the figure) at the pump field strength $30I_0$ (or 33γ, I_0 corresponds to $\Omega_{13}=2\times10^8$ Hz of the pump field intensity as in Ref. [9]); the red dots are the experimental results in Ref. [9]. From the figure, we can know that the detuning frequency of the pump field decides whether the peak is enhanced. At $\Delta_2=-0.34$ GHz (i.e., -1.89γ as noted in the figure; see the figure caption), the right peak is enhanced, which corresponds to $|\beta\rangle$ substate in dressed state picture. However, at $\Delta_2=0.32$ GHz (i.e., 1.78γ) the left peak is enhanced, which corresponds to $|\alpha\rangle$ substate. As the probe field is in the weak region ($\Omega_{12}\ll\gamma$), the x-polarized emission photon from the

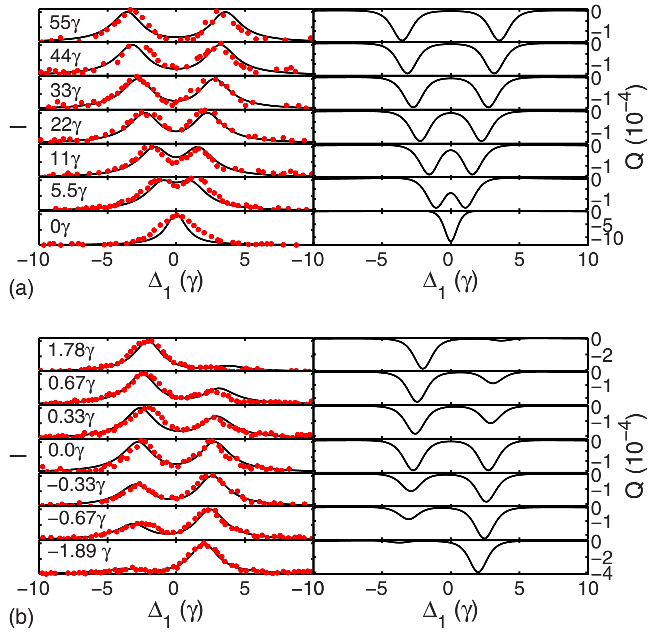

FIG. 2. (Color online) The line shapes and Mandel's Q parameters as a function of detuning frequency of the probe field. The top panel is for different pump field strengths at resonance. The bottom panel is for different detuning frequencies of the pump field at the pump field strength $30I_0$. The red dots are the experimental result in Ref. [9]; the lines are our theoretical results. The parameters are chosen the same with Ref. [9], namely, $\gamma=1.8\times10^8$ Hz, $\Omega_{12}=5\times10^6$ Hz, and $\Omega_{13}=2\times10^8$ Hz. However, for consistency in this paper, we label the coordinate of detuning frequencies Δ_1 in unit of γ.

system almost displays antibunching behaviors. The first moments of our theoretical results (line shapes) are in good agreement with the experimental results [20]. All the parameters we used are the same as those used in the experiment by Xu *et al.* [9] (see the caption of Fig. 2); no fit parameter was introduced.

Physically, because of the influence of the pump field, the "bare" state $|1\rangle$ with pump field produces "dressed states" $|\alpha\rangle$ and $|\beta\rangle$. In this case, the system could be thought as the Λ system (the excited state $|2\rangle$ and the dressed states $|\alpha\rangle$ and $|\beta\rangle$) with the "direct transitions" between the states $|\alpha\rangle$ and $|\beta\rangle$. The transitions between the states $|\alpha\rangle$ and $|\beta\rangle$ depend on the pump field, the lifetime of state $|3\rangle$, and the detuning frequencies of pump field Δ_2. It is the transition between the states $|\alpha\rangle$ and $|\beta\rangle$ that we can see in the two peaks when we count the photons emitted from state $|2\rangle$. For the case of $\Delta_2=0$, the dressed states $|\alpha\rangle$ and $|\beta\rangle$ will be equally excited because of their symmetry, so the two symmetric peaks are obtained (see the top panel of Fig. 2). However, if the detuning frequency Δ_2 scans from -1.89γ (-0.34 GHz) to 1.78γ (+0.32 GHz), the dressed states $|\beta\rangle$ and $|\alpha\rangle$ will be excited differently as shown in bottom panel of Fig. 2.

Figure 3 shows the line shapes and Mandel's Q parameters of the x-polarized photons of the system as a function of the detuning frequency Δ_1 for the pump field $\Omega_{13}=10\gamma$. The different color lines represent the different probe field strengths. From this figure, we can know, at the weak probe field (here is $\Omega_{12}=0.5\gamma$), the line shape is almost the same as

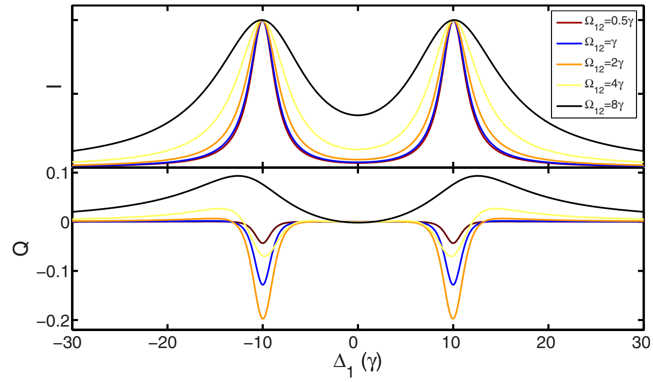

FIG. 3. (Color online) The line shapes and Mandel's Q parameters as a function of the detuning frequency of the probe field. The pump field strength is $\Omega_{13}=20\gamma$ and $\Delta_2=0$.

that of the $\Omega_{12}=\gamma$ (we scaled the line shape). With the increasing probe field, the line shape shows the power broaden effect. Mandel's Q parameters demonstrate the fluctuations of the x-polarized photons from antibunching to bunching as the probe field increases. And at surround of $\Omega_{12}=2\gamma$, Mandel's Q parameter has the minus maximum value. That is, we can modify the statistical properties of the x-polarized photon through changing the probe field strength. $\Omega_{12}=2\gamma$ could be thought as the optimal probe strength to get strong antibunching behaviors of emission photons in this case.

Figure 4 shows the expectation value of the emission x-polarized photon numbers (top panel) and Mandel's Q spectra (bottom panel) of the system as a function of the

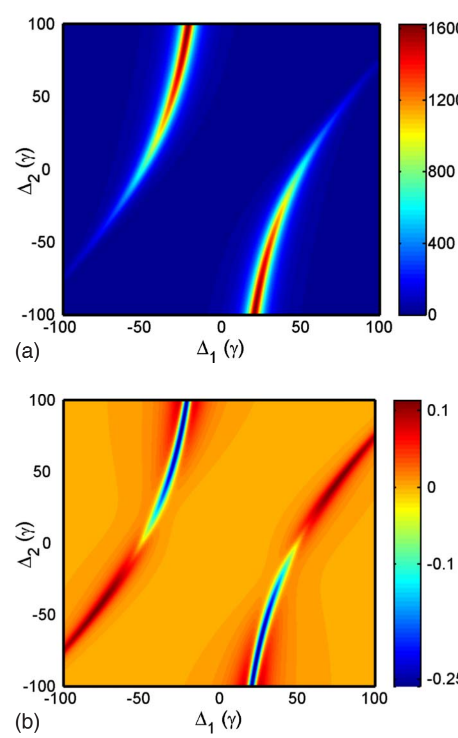

FIG. 4. (Color online) The expectation value of photon numbers and Mandel's Q parameter as a function of the detuning frequency of the pump field Δ_2 and the probe field Δ_1 for long time. The pump and probe field strengths are $\Omega_{13}=100\gamma$ and $\Omega_{12}=5\gamma$, respectively.

detuning frequencies of the pump field Δ_2 and probe field Δ_1 for long time (we use the pump and probe field strengths $\Omega_{13}=100\gamma$ and $\Omega_{12}=5\gamma$, respectively). The figure demonstrates two bands because of Aulter-Townes splitting, which reflects the position of the substates $|\alpha\rangle$ and $|\beta\rangle$. The left band corresponds to the state $|\alpha\rangle$ and the right band corresponds to the state $|\beta\rangle$. Clearly, the peaks of the expectation value of the emission photon numbers in detuning space of Δ_1 and Δ_2 show the properties of the detuning and Rabi frequencies of the pump field, i.e., the peaks of two bands satisfy [15] $\Delta_1=\frac{1}{2}(\Delta_2\pm\sqrt{\Delta_2^2+\Omega_{13}^2})$. Also, the distance of the peaks of two bands in the case of $\Delta_2=0$ gives the strength of the pump field. The symmetry of the peaks of the two bands shows the symmetry of the dressed states about the position of state $|1\rangle$. In the limit of the absence of the pump field, they will "go" together and become one along the Δ_2. The expectation value of the x-polarized photon $\langle N^{(1)}\rangle$ increases as the detuning frequency of the pump field Δ_2 increased in the state $|\alpha\rangle$, but it is not the case to the state $|\beta\rangle$. Mandel's Q parameter varies from the values of positive to negative with the increasing of pump field detuning Δ_2 for the branch of state $|\alpha\rangle$. In this case, Mandel's Q parameter shows that the Δ_1 and Δ_2 can be used to decide the statistical properties of the x-polarized photon emission from the system. For example, at large detuning frequency $\Delta_2=100\gamma$, the properties of the two peaks are different, one shows the antibunching behavior and the other one shows bunching behavior.

The probabilities of emission one-photon, two one-photon processes of x-polarized photons as a function of the time and detuning frequency Δ_1 of the probe field are demonstrated in Fig. 5. The pump and probe field strengths are $\Omega_{13}=15\gamma$ and $\Omega_{12}=2\gamma$, respectively. The detuning frequency of the pump field is $\Delta_2=0$. The top panel of Fig. 5 is the probabilities of emission one photon. At early time, the distributions of the probabilities have two peaks which correspond to the two bands of Aulter-Townes splitting. The probabilities approach the maximum value at time $\gamma t\sim 4$, and each of the peaks splits into two subpeaks and then separates with each other with time evolution. Also this separation is becoming large with the time evolution. The probability of emission two one-photon processes has a maximum value at time $\gamma t\sim 8$, and each of the peaks also splits into two subpeaks with the time evolution. However, the separating distance is smaller than that of one-photon process probability. This means that we could think the probabilities of emission photons as the "onion" structure along the time evolution. That is, the skin of the two one-photon process emission probabilities is within the skin of the one-photon emission probabilities, the skin of the three one-photon process emission probabilities is within the skin of the two one-photon process emission probabilities, etc. This shows that we can first find the one-photon process, then is the two one-photon processes, and the next is the processes of the three one photon. It gives us a way to obtain the one-photon process, two one-photon processes, and so on under the influences of the probe field.

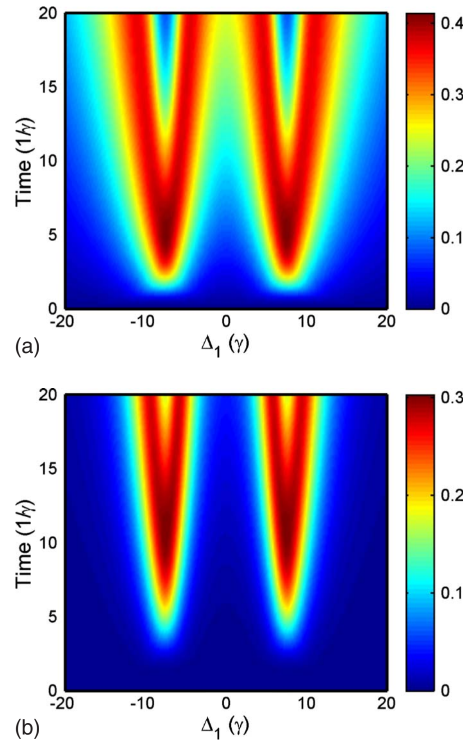

FIG. 5. (Color online) The probabilities of emission one (top panel), two photons (bottom panel) as a function of the detuning frequency probe field and time. The pump and probe field strengths are $\Omega_{13}=15\gamma$ and $\Omega_{12}=2\gamma$, respectively. The detuning frequency of pump is $\Delta_2=0$.

In conclusion, we have presented a theoretical strategy for coherent optical spectroscopy of single QD. We showed the line shapes and Mandel's Q parameters as the detuning frequency of the probe field at different pump intensities and the detuning of the pump field; they agree well with the experimental results. Our theoretical results further show how the detuning frequencies of pump and probe modify the emission photon statistical properties for the cw pump-probe field in this work. Our method allows us to optimize the probe and pump fields to obtain the obvious anitbunching x-polarized photons, and the properties of x-polarized photon can be controlled by the pump and probe fields. Also, our treatment is general and can be beyond the RWA approximation. We can also design the probe and pump fields to obtain the single photon process and two one-photon processes from single QD on demand based on the theoretical framework.

This work was supported by the National Science Foundation of China (Grants No. 10674083 and No. 10874102) and National Basic Research Program of China (Grant No. 2009CB929404). Partial financial support from the Research Fund for the Doctoral Program of Higher Education (Grant No. 200804220004) is acknowledged.

[1] G. C. Hegerfeldt and M. B. Plenio, Quantum Opt. **6**, 15 (1994).
[2] D. A. Cardimona, M. G. Raymer, and J. C. R. Stroud, J. Phys. B **15**, 55 (1982).
[3] T. H. Stievater, X. Li, D. G. Steel, D. Gammon, D. S. Katzer, D. Park, C. Piermarocchi, and L. J. Sham, Phys. Rev. Lett. **87**, 133603 (2001).
[4] N. H. Bonadeo, J. Erland, D. Gammon, D. Park, D. S. Katzer, and D. G. Steel, Science **282**, 1473 (1998).
[5] Z. Ficek and S. Swain, Phys. Rev. A **69**, 023401 (2004).
[6] H. Huang, S. Y. Zhu, M. S. Zubairy, and M. O. Scully, Phys. Rev. A **53**, 1834 (1996).
[7] H. Htoon, T. Takagahara, D. Kulik, O. Baklenov, A. L. Holmes, and C. K. Shih, Phys. Rev. Lett. **88**, 087401 (2002).
[8] D. Gammon, N. H. Bonadeo, G. Chen, J. Erland, and D. G. Steel, Physica E (Amsterdam) **9**, 99 (2001).
[9] X. Xu, B. Sun, P. R. Berman, D. G. Steel, A. S. Bracker, D. Gammon, and L. J. Sham, Science **317**, 929 (2007).
[10] S. H. Autler and C. H. Townes, Phys. Rev. **100**, 703 (1955).
[11] J. Qi, F. C. Spano, T. Kirova, A. Lazoudis, J. Magnes, L. Li, L. M. Narducci, R. W. Field, and A. M. Lyyra, Phys. Rev. Lett. **88**, 173003 (2002).
[12] M. A. Quesada, A. M. F. Lau, D. H. Parker, and D. W. Chandler, Phys. Rev. A **36**, 4107 (1987).
[13] J. Qi, G. Lazarov, X. Wang, L. Li, L. M. Narducci, A. M. Lyyra, and F. C. Spano, Phys. Rev. Lett. **83**, 288 (1999).
[14] Z. Sun and N. Lou, Phys. Rev. Lett. **91**, 023002 (2003).
[15] C. Cohen-Tannoudji, B. Dui, B. Diu, and F. Laloe, *Quantum Mechanics* (Wiley-Interscience, New York, 2006).
[16] S. Mukamel, *Principles of Nonlinear Optical Spectroscopy* (Oxford University Press, Oxford, 1995).
[17] N. G. van Kampen, *Stochastic Processes in Physics and Chemistry* (North-Holland, Amsterdam, 1992).
[18] Y. Zheng and F. L. H. Brown, Phys. Rev. Lett. **90**, 238305 (2003).
[19] S. Mukamel, Phys. Rev. A **68**, 063821 (2003).
[20] It should be noted that our theoretical results agree with the experimental results except for the zero detuning frequency. The reason about the shift is noted in Ref. [9]: "there is a small energy shift of the response relative to the low-intensity excitation that is probably due to a small screening of the applied field by photoexcited charge in the diode."